


# Preparation and characterization of nanocomposites based on PLA and TiO<sub>2</sub> nanoparticles functionalized with fluorocarbons

Antonella Marra<sup>1</sup>  · Clara Silvestre<sup>1</sup> ·  
Aleksandra Porjazoska Kujundziski<sup>2</sup> ·  
Dragica Chamovska<sup>3</sup> · Donatella Duraccio<sup>4</sup>

Received: 6 July 2016 / Revised: 2 November 2016 / Accepted: 8 December 2016 /  
Published online: 18 December 2016  
© Springer-Verlag Berlin Heidelberg 2016

**Abstract** Poly(L-lactic acid)–TiO<sub>2</sub> nanocomposite films were prepared by twin-screw mixer and compression molding. Compatibility between polymer matrix and nanoparticles were improved by modification of the TiO<sub>2</sub> surface with fluorocarbons plasma treatment. 2 and 5 were the % in weight of modified functionalized TiO<sub>2</sub> (fTi) used in this work. Not modified TiO<sub>2</sub> nanoparticles were also used at the same % for comparison. The nanocomposites were analyzed in terms of molecular mass, structure, morphology, thermal stability, mechanical properties and UV absorbance. It was found that TiO<sub>2</sub> nanoparticles affected slightly the PLA molecular weight during mixing and the phenomenon was more marked for functionalized nanoparticles (fTi). All the films presented a good dispersion of nanoparticles in PLA matrix. However, a better interfacial interaction was found for nanocomposites containing modified nanoparticles, and this was reflected in the improved mechanical properties. Moreover, all the nanocomposites showed extension of UV absorption area and increase of the thermal stability. Both UV adsorption and thermal stability increased by increasing TiO<sub>2</sub> content and at a given composition for nanocomposites containing modified TiO<sub>2</sub>.

---

✉ Antonella Marra  
antonella.marra@ipcb.cnr.it

<sup>1</sup> Istituto per i Polimeri, Compositi e Biomateriali (IPCB)-CNR, via Campi Flegrei 34, 80078 Pozzuoli, Naples, Italy

<sup>2</sup> Faculty of Engineering, International Balkan University, Samoilova 10, 1000 Skopje, Republic of Macedonia

<sup>3</sup> Faculty of Technology and Metallurgy, Sts. Cyril and Methodius University, Boulervad Goce Delchev 9, 1000 Skopje, Republic of Macedonia

<sup>4</sup> Istituto per le Macchine Agricole e Movimento Terra (IMAMOTER)-CNR, Strada delle Cacce 73, 10135 Turin, Italy

**Keywords** Biopolymers and renewable polymers · Nanoparticles · Properties and characterization · Mechanical properties · Thermogravimetric analysis (TGA)

## Introduction

Conventional polymer materials are produced mostly from fossil fuels and their disposal by incineration produces carbon dioxide emission and contributes to global warming and pollution. Thus, the development of polymers made from sustainable and renewable sources is growing at a rapid rate. Poly(lactide), PLA, as a biodegradable polymer, has attracted a big attention from both fundamental and practical perspectives. In fact it can be synthesized by chemical synthesis from bio-derived monomers and is environmentally and economically appropriate [1–3]. PLA has potential for use in a wide range of applications and commercially available products are already on the market [4]. Initially, the high production cost confined the PLA applications to biomedical sector such as material for bioabsorbable surgical sutures and implants, for drug delivery systems [5, 6], scaffolds for growth and proliferation of cells [7, 8]; however, the new production technology [4] decreased its cost and enlarged its range of applications, such as for disposable products (baby diapers and plastic bags), as well as for traditional applications in substitution of traditional thermoplastics for instance, industrial devices, packaging films and fiber materials [4, 9, 10]. However, to further increase PLA applications, some properties such as thermal stability, mechanical properties, barrier properties, need to be improved [11].

Many different techniques, such as copolymerization [12, 13], preparation of composites [14, 15], etc., have been applied for improving some PLA properties. Anyway, the most successful practice, as reported in literature, is the preparation of nanocomposites with various fillers [16–36] such as clays [21–27], silica [28] carbon based nanoparticles [29–32], metal oxides [17, 19, 33, 34] and polysaccharide nanofillers [35, 36]. Among them, titanium dioxide ( $\text{TiO}_2$ ) is a very important chemical and environmental material. Nano- $\text{TiO}_2$  particles possess many good properties such as attractive photocatalytic activity, chemical reactivity, excellent photostability, biocompatibility and relevant antimicrobial activity [34, 37, 38]. Most investigations about PLA/ $\text{TiO}_2$  nanocomposites have mainly been dedicated to the analysis of the influence of nanoparticles on photo-degradability [19], toughness [39], kinetics of crystallization [40] and the drug-releasing in target cancer cells of PLA [41].

According to literature data the direct mixing of  $\text{TiO}_2$  with PLA yields to the formation of large nanoparticles aggregates into the polymer matrix. In this context, some surface treatments of  $\text{TiO}_2$  nanoparticles were reported to improve their dispersion into the PLA as matrix [19, 42–44].

The aim of this article is twofold: (1) to report the study on the optimization of the conditions for the modification of  $\text{TiO}_2$  surface using perfluorocarbons through plasma treatment and for the preparation of PLA/ $\text{TiO}_2$  nanocomposites films at 2 and 5 wt%  $\text{TiO}_2$  through melt mixing followed by compression molding; (2) to

investigate the properties of the films in terms of molecular mass, structure, morphology, thermal stability, mechanical properties and UV absorbance.

## Experimental

### Materials

Poly(L,L-lactide), PLA 4032 D ( $M_n = 1.3 \times 10^5$  g/mol,  $M_w = 2.1 \times 10^5$  g/mol, density = 1.24 g/cm<sup>3</sup>) was provided by NatureWorks, USA. Hydrophilic titanium dioxide TiO<sub>2</sub> (Ti) nanoparticles (P-25 standard, 99.5% purity, with average particle size 25 nm, 80% anatase and 20% rutile) were obtained from Degussa, Germany. Fluorocarbon functionalized TiO<sub>2</sub> nanoparticles (fTi) were supplied by University of Texas Arlington.

### Functionalization of TiO<sub>2</sub> nanoparticles

Fluorocarbon functionalized TiO<sub>2</sub> nanoparticles (fTi) were used for increasing the compatibility between particles and PLA and also for enhancing their dispersion in the polymer matrix. The functionalization has been obtained using plasma treatment. The reactor details are similar to that previously described [45]. The plasma was generated using RF (13.56 MHz frequency) power input. Initially the TiO<sub>2</sub> nanoparticles underwent to a brief, high power O<sub>2</sub> plasma discharge to remove any adsorbed carbonaceous materials and, simultaneously, to activate their surfaces. Immediately following the oxygen treatment, the perfluorocarbon monomer was introduced and a high power continuous wave plasma discharge was employed briefly (1 min) to graft a thin, strongly adherent, amorphous carbon-like layer to the TiO<sub>2</sub> particles. The function of this layer is to overcome the inherent chemical incompatibility between the inorganic particles and the plasma deposited organic films. Subsequently, the RF power input was converted to a pulse operational mode and the plasma duty cycle, i.e., ratio of plasma on to plasma off times, was slowly decreased, thus creating a gradient layered structure in which the fluorine content of the plasma polymer film is slowly increased as the pulsed plasma duty cycle is decreased. The process was terminated at a plasma duty of 10 ms on and 100 ms off and peak power input of 200 W. The final *F/C* reached 2.1/1 measured by FTIR and XPS spectra [45].

### Nanocomposites preparation

Before mixing, TiO<sub>2</sub> and PLA were dried in an oven for 24 h at 65 °C under vacuum. PLA was mixed with TiO<sub>2</sub> powder using a torque rheometer Brabender Plastograph EC (Kulturstr, Duisburg, Germany) at a screw speed of 50 rpm and mixing temperature of 180 °C for 15 min. Two formulations were prepared: 2 and 5 wt% of neat (from this point they will be referred as PLATi2, PLATi5) and functionalized TiO<sub>2</sub> (from this point PLAfTi2 and PLAfTi5). Neat PLA was

processed in such a way so that all the samples analyzed have the same thermal history.

Films were obtained by compression molding in a press Dr. Collin GmbH P200E (Ebersberg, Germany) at a temperature of 180 °C for about 6 min, without any additional pressure, to allow complete melting of the material. Subsequently the pressure was increased up to 100 bars and kept constant for about 3 min. The press is equipped with water cooling system which brings the system to room temperature in about 5 min. Pure PLA and nanocomposites films have been prepared with the thickness of about 150 μm.

## Characterization

### *Attenuated total reflection spectroscopy (ATR)*

ATR spectra of nanoparticles were recorded after drying at 65 °C for 24 h to verify the chemical link nature between the nanoparticles and fluorocarbon layer. Samples were prepared as KBr pellets and scanned against a blank KBr pellet background at wave numbers ranging from 4000 to 400 cm<sup>-1</sup> with resolution of 4.0 cm<sup>-1</sup> through the accumulation of 8 scans using a Perkin Elmer Spectrum 100 (Shelton, Connecticut, USA).

### *Gel permeation chromatography (GPC)*

It was performed on GPC-150C Waters Chromatography instrument (Milford, Massachusetts, USA) equipped with two linear columns Polymer Laboratories and elution with tetrahydrofuran (THF). The flow rate was 1 ml/min. The eluent was monitored by PL-ELS 2100 detector. Molecular weights and molecular weight distributions were calculated by reference to a PS standard calibration curve, with the Kuhn–Mark–Houwink equation for poly(L-lactide) in THF:  $M_n(\text{PLA}) = 0.4055 \times M_n(\text{PS})^{1.0486}$  [46].

### *Wide-angle X-ray diffraction (WAXD)*

Measurements were performed using a Philips XPW diffractometer (Philips Analytical, Almelo, The Netherlands) with Cu K $\alpha$  radiation (1.542 Å) filtered by nickel. The scanning rate was 0.02 °C/min and the scanning angles were from 5° to 45°.

### *Scanning electron microscopy (SEM)*

The analysis was performed using a Fei Quanta 200 FEG electron scanning microscope (Hillsboro, Oregon-USA) on cryogenically fractured surfaces. Before the observation, samples were coated with a Au/Pd alloy using an E5 150 SEM coating unit.

### *Differential scanning calorimetry (DSC)*

The thermal behaviour of the nanocomposites was examined by differential scanning calorimetry (DSC) using a calorimeter TA Q2000 (Milano, Italy). DSC measurements were carried out by heating samples from 25 to 200 °C at a rate of 2 °C/min. Heat fusion and temperature were calibrated with an indium standard and background subtraction was done by TA instruments protocols.

### *Thermogravimetric analysis (TGA)*

The thermal stability of the nanocomposites was examined by thermogravimetric analysis (TGA) using a Perkin Elmer-Pyris Diamond apparatus (Boston, Massachusetts-USA) with a heating rate of 20 °C/min in air.

### *Mechanical properties*

The films for tensile tests were cut in the form of dumbbell width of 0.4 cm, according to ASTM (D368), using a die steel. Stress–strain curves were obtained using an Instron dynamometer, model 4505 (Pianezza, Torino, Italy), the tests were carried out at room temperature (25 °C) and at a cross-head speed of 5 mm/min. Twenty tests were performed for each sample.

### *UV–visible spectrophotometry*

UV–visible spectra of PLA and nanocomposites were monitored with Jasco V-570 (Cremella, Como-Italy) spectrophotometer in the range between 200 and 900 nm at 50 nm per step.

## **Results and discussion**

### **Characterisation of TiO<sub>2</sub> nanoparticles**

In Fig. 1 the ATR nanoparticles spectra are reported in the range between 1500 and 400 cm<sup>-1</sup>. Ti nanoparticles give no peak around 1500 and 1000 cm<sup>-1</sup>, while when they are functionalized by fluorocarbons, a new broad vibrational band is visible. It arises from the fluorocarbon sequences (–CF<sub>2</sub>–)<sub>n</sub>, e.g., the symmetric [ $\nu_s$ (CF<sub>2</sub>)] and the antisymmetric [ $\nu_{as}$ (CF<sub>2</sub>)] CF<sub>2</sub> stretching modes at about 1226 and 1140 cm<sup>-1</sup>, respectively. Distinct peaks are not well visible due to the heterogeneity of the surface adsorption sites [47]. Anyway they are well known as characteristic features in spectra of perfluoroalkanes and poly(tetrafluoroethylene) (PTFE) [48]. The infrared adsorption bands between 400 and 800 cm<sup>-1</sup> are assigned to the vibrations of Ti–O and Ti–O–Ti framework bonds [49]. From IR spectroscopy, it is possible to confirm that TiO<sub>2</sub> nanoparticles are indeed functionalized by perfluorocarbons that will adsorb on TiO<sub>2</sub> via the surface hydroxyl groups.

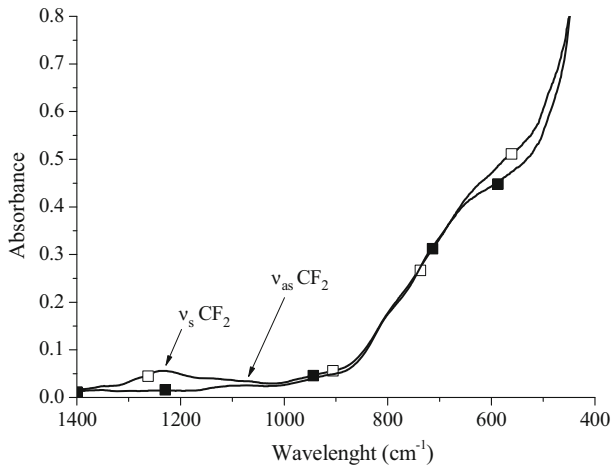


**Fig. 1** ATR spectra of bare (filled squares) and functionalized (open squares) TiO<sub>2</sub> nanoparticles

## GPC

PLA is known to rapidly degrade when melted at high temperatures, losing from 20 to 80% of its initial  $M_n$  on melt processing [46, 50]. It was, therefore, interesting to compare the effect of filler incorporation on the evolution of  $M_n$  with thermal treatment. Table 1 shows the molecular parameters of unfilled PLA and nanocomposites after mixing and after compression molding. The mixing does not seem to affect the molecular weight of neat PLA and the following process step of compression molding induces a decrease in  $M_n$  of 22.3%. This result can be probably ascribed to the presence of a stabilizer in the commercial PLA and to the mild processing condition used in this work. The introduction of TiO<sub>2</sub> nanoparticles only slightly affects the PLA molecular weight during mixing due to some hydrolysis at high temperature. PLA degradation increases by increasing the amount

**Table 1** Molecular parameters for the PLA and nanocomposites after mixing (mix) and after compression molding (film)

	$M_n \times 10^{-4a}$	$M_w \times 10^{-4a}$	$M_w/M_n$
PLA <sub>pellet</sub> <sup>b</sup>	13.0	21.0	1.61
PLA <sub>mix</sub>	13.3	20.8	1.56
PLATi2 <sub>mix</sub>	13.1	22.3	1.70
PLATi2 <sub>mix</sub>	13.0	21.9	1.68
PLATi5 <sub>mix</sub>	12.8	21.6	1.69
PLATi5 <sub>mix</sub>	12.0	20.3	1.69
PLA <sub>film</sub>	10.1	15.5	1.54
PLATi2 <sub>film</sub>	9.7	14.3	1.47
PLATi2 <sub>film</sub>	8.2	12.6	1.54
PLATi5 <sub>film</sub>	9.5	14.7	1.54
PLATi5 <sub>film</sub>	9.3	14.7	1.58

<sup>a</sup> Calculated by reference to a PS standard calibration curve with the Kuhn–Mark–Houwink equation for PLA in THF:  $M_n$  (PLA) =  $0.4055 \times M_n$  (PS)<sup>1.0486</sup> [46]

<sup>b</sup> Data obtained from the manufacturer

of nanoparticles and the phenomenon is more marked for functionalized nanoparticles (fTi). The maximum  $M_n$  reduction of 9.8% was observed for PLA/Ti<sub>5</sub> mix respect to PLA<sub>mix</sub>. The compression molding process further reduces the PLA molecular weight in all the nanocomposites. Anyway the  $M_n$  reduction of nanocomposites is not so high and varies in the range from 4 to 18% respect to PLA<sub>film</sub> and from 27 to 38% respect to PLA<sub>mix</sub> in accordance with other results found in literature for PLA nanocomposites [51, 52].

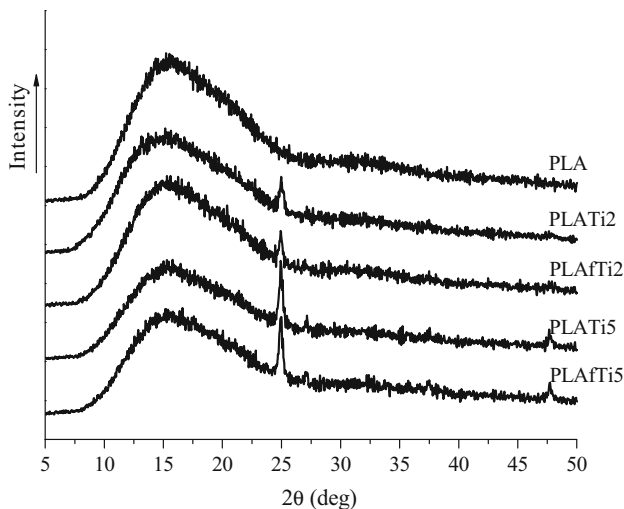
### Structure and morphology of nanocomposites

WAXD profiles of PLA and its nanocomposites are reported in Fig. 2. All the samples are amorphous. TiO<sub>2</sub> does not affect the crystallization process of PLA during the preparation of films in the condition used in this work. The observed reflection at  $2\theta = 25.3^\circ$  in the nanocomposite profile corresponded to the (101) reflection of anatase phase of TiO<sub>2</sub> nanoparticles [53].

SEM micrographs reported in Fig. 3 clearly show that nanoparticles are well dispersed in PLA film. Their distribution is quite uniform and homogeneous and no aggregate phenomena are visible even at higher TiO<sub>2</sub> compositions.

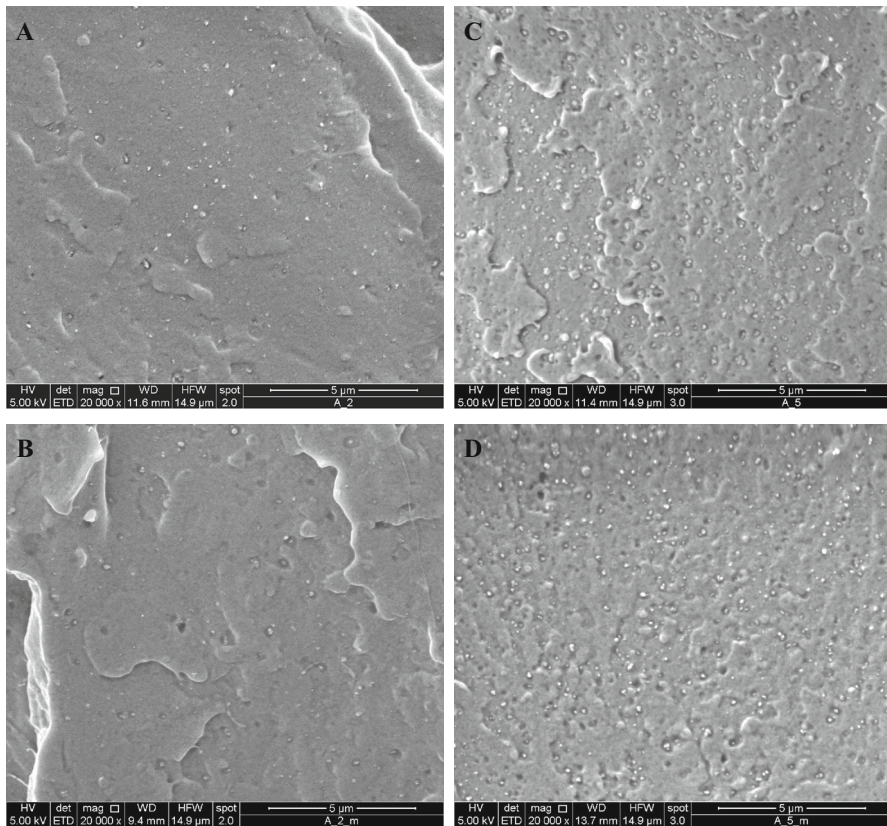
### Thermal analysis

Figure 4 shows the DSC thermograms of PLA and nanocomposite film in the first heat scan. The addition of bare and functionalized TiO<sub>2</sub> in PLA does not result in a noticeable change in the glass transition (61 °C) of PLA. The cold crystallization temperature ( $T_{cc} = 94$  °C) does not depend on the TiO<sub>2</sub> content, this suggests that small-size particles are dispersed enough in the PLA matrix, and that only a small amount of them serves well as a nucleating agent. Similar results can be found in



**Fig. 2** WAXD spectra of neat PLA and its nanocomposites





**Fig. 3** Scanning electron micrographs of PLATi2 (a), PLAfti2 (b), PLATi5 (c) and PLAfti5 (d) films fractured in liquid nitrogen, at a magnification of 20,000 $\times$

other PLA nanocomposites [43, 54, 55]. Moreover, all the thermograms present an exothermic shoulder before melting at about 153 °C which is function of the process conditions and DSC heating program and that can be attributed to the recrystallization of disordered  $\alpha'$ -crystals into  $\alpha$  form [56, 57]. The  $\alpha$  form melts at 169 °C in all the nanocomposites indicating that also this process is not affected by the TiO<sub>2</sub> nanoparticles.

### Thermogravimetric analysis

The thermogravimetric curves of all samples and their derivative (DTG) are shown in Fig. 5a, b, respectively. TD<sup>i</sup> and T<sub>max</sub> that are the temperature at a 5% weight loss and at the maximum of the derivative curves, respectively, are reported in Table 1. PLA depolymerization by back-biting (chain end scission or intramolecular transesterification) occurs in the range from 289 to 340 °C [58]. For the nanocomposites, the initial degradation temperature (TD<sup>i</sup>) increases with the increasing amount of TiO<sub>2</sub> with a maximum of 10 °C from the value of pure PLA



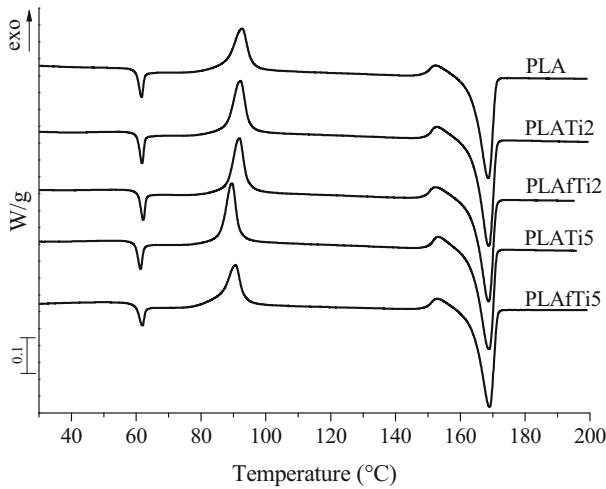


**Fig. 4** DSC curves (IRUN) for PLA and PLA/TiO<sub>2</sub> nanocomposites, heating rate of 2°C/min

for 5% TiO<sub>2</sub>. Moreover, at the same TiO<sub>2</sub> loading, TD<sup>i</sup> is higher for nanocomposites containing fTi respect to that of nanocomposites containing Ti. The same trend is found for  $T_{max}$  as can be seen in Table 2. Because inorganic species have good thermal stabilities, it is generally believed that the introduction of inorganic components into organic materials can improve their thermal stabilities. This increase can be attributed to the high thermal stability of TiO<sub>2</sub> and to the interaction between the TiO<sub>2</sub> particles and the polymer matrix. The same results have been found for other nanocomposites [59–62]. However, opposite behaviour has also been found [63].

As it can be seen from DTG curves, only for PLAfTi2 and PLAfTi5 the global degradation process is shifted to higher temperatures respect to neat PLA. PLATi2 and PLATi5 nanocomposites shows sharper DTG curves respect to PLA and nanocomposites containing fTi. This result indicates that when the TiO<sub>2</sub> nanoparticles are not functionalized, they hinder the degradation of PLA at low temperatures, but also act as degradation accelerators at higher temperatures.

### Tensile properties

Neat PLA exhibits yielding with a short quasi-constant stress regime and failed at ca. 6.1% (Fig. 6; Table 2). The specimen yields with stress-whitening bands. All neat PLA specimens fracture without necking. In PLATi nanocomposites, yield and break parameters decrease with Ti loading and more visually observable stress whitening in the specimen is observable. On the other hand, Young's modulus shows a slight increase with Ti. Conversely, the addition of fTi to PLA results in a slight increase in yield stress. The nanocomposites PLAfTi show intense stress whitening resulting in a large yielding regime and hence significant strain-at break (ca. 9.3% at 2 wt% fTi and ca. 14.5 at 5 wt% fTi). Young's modulus increases with fTi concentration. These results clearly indicate that PLA chain have a good

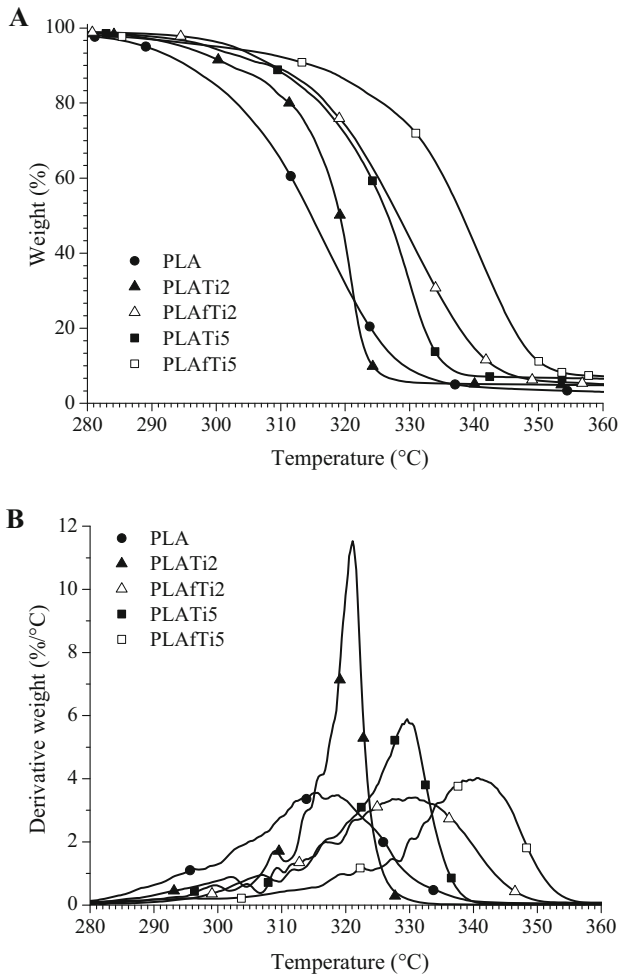


**Fig. 5** TGA (a) and DTG (b) of PLA, PLATi2, PLATi5, PLAFti2 and PLAFti5 nanocomposites recorded at 20 °C/min in air

compatibility and strong interfacial interaction with fTi that increase stress transfer to the fTi nanoparticles resulting in high tensile parameters.

### UV–visible spectrophotometry

UV–vis measurements are carried out to study the optical transparency of the nanocomposites and the UV barrier due to the presence of TiO<sub>2</sub> nanoparticles in the polymer matrix. Figure 7 shows the UV–vis transmittance spectra of the neat PLA and nanocomposites. The neat polymer shows the highest UV–vis transmittance. In the visible region PLA film has a transmittance of about 76%, the PLA transmittance starts to decrease at about 382 nm and becomes 0 at 225 nm; this

**Table 2** Thermal degradation temperatures and tensile parameters for PLA and PLA/TiO<sub>2</sub> nanocomposites

	TD <sup>i</sup> (°C)	T <sub>max</sub> (°C)	ε <sub>y</sub> (%)	σ <sub>y</sub> (MPa)	ε <sub>b</sub> (%)	σ <sub>b</sub> (MPa)	E (MPa)
PLA	289 ± 1	317 ± 1	1.3 ± 0.17	34.9 ± 5.6	5.7 ± 0.4	28.3 ± 4.7	3100.2 ± 131.7
PLATi2	295 ± 1	319 ± 1	1.1 ± 0.14	29.1 ± 4.0	5.0 ± 0.5	24.4 ± 2.1	3465.8 ± 276.2
PLATi5	303 ± 1	331 ± 1	1.2 ± 0.11	30.7 ± 4.7	4.4 ± 0.3	22.9 ± 3.1	3599.0 ± 228.1
PLAFti2	299 ± 1	328 ± 1	1.4 ± 0.13	39.3 ± 3.9	10.1 ± 0.5	30.4 ± 3.3	3225.2 ± 181.7
PLAFti5	300 ± 1	344 ± 1	1.4 ± 0.13	41.4 ± 4.7	14.5 ± 0.7	30.7 ± 2.4	3395.8 ± 201.5

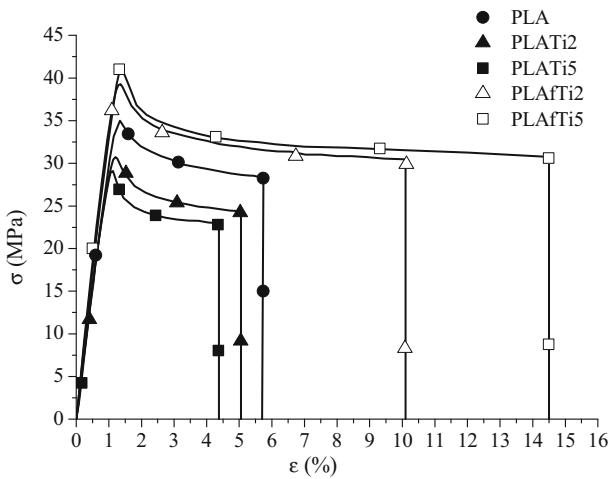


**Fig. 6** Stress-strain curves of PLA, PLATi and PLAFti nanocomposites

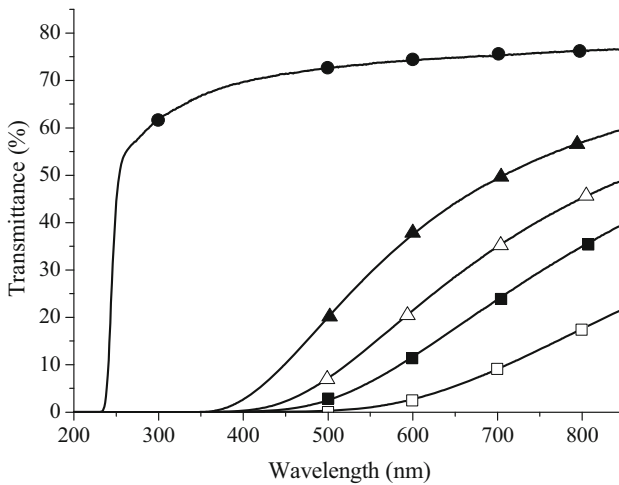


**Fig. 7** UV–visible spectrum of PLA (filled circles), PLATi2 (filled triangles), PLATi5 (filled squares), PLAFti2 (open triangles) and PLAFti5 (open squares) film nanocomposites

saturation of the spectra at 225 nm is due to the absorbance of PLA ester groups [64]. Increases in the light adsorption (reductions in transmittance) in both visible and UV ranges are observed with the increase of the concentration of TiO<sub>2</sub>. This effect is even more evident in the nanocomposites containing fTi. The transmittance reaches 0% at higher wavelength by increasing the TiO<sub>2</sub> content. Again, by comparing spectra with the same TiO<sub>2</sub> content, the saturation is reached at higher wavelength for fTi respect to Ti. These results indicate that the scale of TiO<sub>2</sub> inclusions (both bare and functionalized) is probably large enough to scatter visible light. Furthermore, TiO<sub>2</sub> nanoparticles, in particular when they are functionalized with fluorocarbons extend the UV absorption area.

## Conclusions

The aim of this work was to study the influence of functionalised nanoparticles on the molecular weight, structure, morphology, thermal, mechanical and UV properties of PLA. Modified TiO<sub>2</sub> nanoparticles were functionalized with fluorocarbons by plasma treatment. PLA/TiO<sub>2</sub> nanocomposites were obtained by melt mixing and the films were prepared by compression moulding.

TiO<sub>2</sub> nanoparticles (both Ti and fTi) did not affect the crystallization process and the thermal parameters of PLA during the film preparation in the condition used in this work: all the nanocomposites were amorphous and had same  $T_g$ ,  $T_{cc}$  and  $T_m$ .

The morphological analysis has evidenced that the functionalization of TiO<sub>2</sub> nanoparticles with fluorocarbons plasma treatment improved their dispersion into the PLA matrix that leads to samples that present improved mechanical properties (higher break parameters and toughness), thermostability and a larger UV absorption area. The improvement of these properties is more evident for the higher content of fTi nanoparticles (i.e., 5 wt%).

**Acknowledgements** Professor Richard B. Timmons of University of Texas, Arlington, USA is thanked for supplying fluorocarbon TiO<sub>2</sub> nanoparticles functionalized by plasma treatment. Dr. Barbara Immirzi of the Istituto per i Polimeri, Compositi e Biomateriali(CNR), Pozzuoli(NA), Italy is thanked for performing GPC analysis.

## References

1. Grijpma DW, Pennings AJ (1994) (Co)polymers of L-lactide, 2. Mechanical properties. *Macromol Chem Phys* 195:1649–1663. doi:[10.1002/macp.1994.021950516](https://doi.org/10.1002/macp.1994.021950516)
2. Cheng Y, Deng S, Chen P, Ruan R (2009) Polylactic acid (PLA) synthesis and modifications: a review. *Front Chem China* 4:259–264. doi:[10.1007/s11458-009-0092-x](https://doi.org/10.1007/s11458-009-0092-x)
3. Liang H, Hao Y, Bian J, Zhang H, Dong L, Zhang H (2015) Assessment of miscibility, crystallization behaviors, and toughening mechanism of polylactide/acrylate copolymer blends. *Polym Eng Sci* 55:386–396. doi:[10.1002/pen.23893](https://doi.org/10.1002/pen.23893)
4. Jamshidian M, Tehrani EA, Imran M, Jacquot M, Desobry S (2010) Poly-lactic acid: production, applications, nanocomposites, and release studies. *Compr Rev Food Sci Food Saf* 9:552–571. doi:[10.1111/j.1541-4337.2010.00126.x](https://doi.org/10.1111/j.1541-4337.2010.00126.x)
5. Dimitrov Ph, Porjazoska A, Novakov Ch, Cvetkovska M, Tsvetanov ChB (2005) Functionalized micelles from new ABC polyglycidol-poly(ethylene oxide)-poly(d,l-lactide) terpolymers. *Polymer* 46:6820–6828. doi:[10.1016/j.polymer.2005.06.002](https://doi.org/10.1016/j.polymer.2005.06.002)

6. Porjazoska A, Goracinova K, Mladenovska K, Glavaš M, Simonovska M, Janjević EI, Cvetkovska M (2004) Poly(lactide-*co*-glycolide) microparticles as systems for controlled release of proteins—preparation and characterization. *Acta Pharm* 54:215–229
7. Porjazoska A, Cvetkovska M, Yılmaz OK, Baysal K, KayamanApohan N, Baysal BM (2004) Synthesis and characterization of biocompatible multicomponent polymer systems as supports for cell cultures. *Bull Chem Technol Macedonia* 23:147–156
8. Porjazoska A, Yılmaz OK, Baysal K, Cvetkovska M, Sirvanci S, Ercan F, Baysal BM (2006) Synthesis and characterization of poly(ethylene glycol)-poly(D,L-lactide-*co*-glycolide) poly(ethylene glycol) tri-block co-polymers modified with collagen: a model surface suitable for cell interaction. *J Biomater Sci Polym Ed* 17:323–340
9. Fukushima K, Fina A, Geobaldo F, Venturello A, Camino G (2012) Properties of poly(lactic acid) nanocomposites based on montmorillonite, sepiolite and zirconium phosphonate. *Express Polym Lett* 6:914–926. doi:[10.3144/expresspolymlett.2012.97](https://doi.org/10.3144/expresspolymlett.2012.97)
10. Darder M, Aranda P, Ruiz-hitzky E (2007) Bionanocomposites: a new concept of ecological, bioinspired, and functional hybrid materials. *Adv Mater* 19:1309–1319. doi:[10.1002/adma.200602328](https://doi.org/10.1002/adma.200602328)
11. Jia S, Qu J, Chen R, Wu C, Huang Z, Zhai S, Liu W, Feng Y (2014) Effects of thermoplastic polyurethane on the properties of poly(lactic acid)/organo-montmorillonite nanocomposites based on novel vane extruder. *Polym Eng Sci* 54:2292–2300. doi:[10.1002/pen.23781](https://doi.org/10.1002/pen.23781)
12. Li Y, Shimizu H (2009) Improvement in toughness of poly(l-lactide) (PLLA) through reactive blending with acrylonitrile–butadiene–styrene copolymer (ABS): morphology and properties. *Eur Polym J* 45:738–746. doi:[10.1016/j.eurpolymj.2008.12.010](https://doi.org/10.1016/j.eurpolymj.2008.12.010)
13. Zhen W, Li J, Xu Y (2014) In situ intercalation green polymerization, characterization, and kinetics of poly(lactic acid)/zinc oxide pillared saponite nanocomposites. *Polym Compos* 35:1023–1030. doi:[10.1002/pc.22748](https://doi.org/10.1002/pc.22748)
14. Najafi N, Heuzey MC, Carreau PJ (2012) Crystallization behavior and morphology of polylactide and PLA/clay nanocomposites in the presence of chain extenders. *Polym Eng Sci* 53:1053–1064. doi:[10.1002/pen.23355](https://doi.org/10.1002/pen.23355)
15. Shahlari M, Lee S (2012) Mechanical and morphological properties of poly(butylene adipate-*co*-terephthalate) and poly(lactic acid) blended with organically modified silicate layers. *Polym Eng Sci* 52:1420–1428. doi:[10.1002/pen.23082](https://doi.org/10.1002/pen.23082)
16. Silvestre C, Duraccio D, Cimmino S (2011) Food packaging based on polymer nanomaterials. *Prog Polym Sci* 36:1766–1782. doi:[10.1016/j.progpolymsci.2011.02.003](https://doi.org/10.1016/j.progpolymsci.2011.02.003)
17. Raquez JM, Habibi Y, Murariu M, Dubois P (2013) Poly(lactide) (PLA)-based nanocomposites. *Prog Polym Sci* 38:1504–1542. doi:[10.1016/j.progpolymsci.2013.05.014](https://doi.org/10.1016/j.progpolymsci.2013.05.014)
18. Petchwattana N, Covavisaruch S, Petthai S (2014) Influence of talc particle size and content on crystallization behavior, mechanical properties and morphology of poly(lactic acid). *Polym Bull* 71:1947–1959. doi:[10.1007/s00289-014-1165-7](https://doi.org/10.1007/s00289-014-1165-7)
19. Nakayama N, Hayashi T (2007) Preparation and characterization of poly(l-lactic acid)/TiO<sub>2</sub> nanoparticle nanocomposite films with high transparency and efficient photodegradability. *Polym Degrad Stab* 92:1255–1264. doi:[10.1016/j.polymdegradstab.2007.03.026](https://doi.org/10.1016/j.polymdegradstab.2007.03.026)
20. Silvestre C, Pezzuto M, Duraccio D, Marra A, Cimmino S (2014) Exploiting nanotechnology and radiation technologies to develop new eco-sustainable nanomaterials for food packaging suitable for sterilization by irradiation. In: IAEA-TECDOC-1745 (ed) Radiation processed materials in products from polymers for agricultural applications. IAEA, Vienna, pp 99–104
21. Rasal RM, Janorkar AV, Hirt DE (2010) Poly(lactic acid) modifications. *Prog Polym Sci* 35:338–356. doi:[10.1016/j.progpolymsci.2009.12.003](https://doi.org/10.1016/j.progpolymsci.2009.12.003)
22. Pluta M, Paul MA, Alexandre M, Dubois P (2006) Plasticized polylactide/clay nanocomposites. I. The role of filler content and its surface organo-modification on the physico-chemical properties. *J Polym Sci Part B Polym Phys* 44:299–311. doi:[10.1002/polb.20694](https://doi.org/10.1002/polb.20694)
23. Pluta M (2006) Melt compounding of polylactide/organo-clay: structure and properties of nanocomposites. *J Polym Sci Part B Polym Phys* 44:3392–3405. doi:[10.1002/polb.20957](https://doi.org/10.1002/polb.20957)
24. Fukushima K, Murariu M, Camino G, Dubois P (2010) Effect of expanded graphite/layered-silicate clay on thermal, mechanical and fire retardant properties of poly(lactic acid). *Polym Degrad Stab* 95:1063–1076. doi:[10.1016/j.polymdegradstab.2010.02.029](https://doi.org/10.1016/j.polymdegradstab.2010.02.029)
25. Sinha Ray S, Yamada K, Okamoto M, Fujimoto Y, Ogami A, Ueda K (2003) New polylactide/layered silicate nanocomposites. 5. Designing of materials with desired properties. *Polymer* 44:6633–6646. doi:[10.1016/j.polymer.2003.08.021](https://doi.org/10.1016/j.polymer.2003.08.021)

26. Haand JU, Xanthos M (2010) Novel modifiers for layered double hydroxides and their effects on the properties of polylactic acid composites. *Appl Clay Sci* 47:303–310. doi:[10.1016/j.clay.2009.11.033](https://doi.org/10.1016/j.clay.2009.11.033)
27. Mohapatra AK, Mohanty S, Nayak SK (2012) Poly(lactic acid) and layered silicate nanocomposites prepared by melt mixing: thermomechanical and morphological properties. *Polym Compos* 33:2095–2104. doi:[10.1002/pc.22316](https://doi.org/10.1002/pc.22316)
28. Li Y, Han C, Bian J, Han L, Dong L, Gao G (2012) Rheology and biodegradation of polylactide/silica nanocomposites. *Polym Compos* 33:1719–1727. doi:[10.1002/pc.22306](https://doi.org/10.1002/pc.22306)
29. Zhao YQ, Lau KT, Li HL (2008) Manufacture of a homogenous nano-diamond/poly (lactic acid) bio-engineered composite. *Adv Mater Res* 47:1221–1224. [www.scientific.net/AMR.47-50.1221](http://www.scientific.net/AMR.47-50.1221)
30. Chrissafis K, Paraskevopoulos K, Jannakoudakis A, Beslikasand T, Bikiaris D (2010) Oxidized multiwalled carbon nanotubes as effective reinforcement and thermal stability agents of poly(lactic acid) ligaments. *J Appl Polym Sci* 118:2712–2721. doi:[10.1002/app.32626](https://doi.org/10.1002/app.32626)
31. Wu D, Wu L, Zhang M, Zhao Y (2008) Viscoelasticity and thermal stability of polylactide composites with various functionalized carbon nanotubes. *Polym Degrad Stab* 93:1577–1584. doi:[10.1016/j.polyimdegradstab.2008.05.001](https://doi.org/10.1016/j.polyimdegradstab.2008.05.001)
32. Murariu M, Dechief AL, Bonnaud L, Paint Y, Gallos A, Fontaine G, Bourbigot S, Dubois P (2010) The production and properties of polylactide composites filled with expanded graphite. *Polym Degrad Stab* 95:889–900. doi:[10.1016/j.polyimdegradstab.2009.12.019](https://doi.org/10.1016/j.polyimdegradstab.2009.12.019)
33. Murariu M, Paint Y, Murariu O, Raquez JM, Bonnaud L, Dubois P (2015) Current progress in the production of PLA–ZnO nanocomposites: beneficial effects of chain extender addition on key properties. *J Appl Polym Sci* 132:42480. doi:[10.1002/app.42480](https://doi.org/10.1002/app.42480)
34. Zhuang W, Liu J, Zhang JH, Hu BX, Shen J (2009) Preparation, characterization, and properties of TiO<sub>2</sub>/PLA nanocomposites by in situ polymerization. *Polym Compos* 30:1074–1080. doi:[10.1002/pc.20658](https://doi.org/10.1002/pc.20658)
35. Jonooi M, Harun J, Mathew AP, Oksman K (2010) Mechanical properties of cellulose nanofiber (CNF) reinforced polylactic acid (PLA) prepared by twin screw extrusion. *Compos Sci Technol* 70:1742–1747. doi:[10.1016/j.compscitech.2010.07.005](https://doi.org/10.1016/j.compscitech.2010.07.005)
36. Wang B, Sain M (2007) The effect of chemically coated nanofiber reinforcement on biopolymer based nanocomposites. *BioResources* 2:371–388
37. Copinet A, Bertrand C, Longieras A, Coma V, Couturier Y (2003) Photodegradation and biodegradation study of a starch and poly(lactic acid) coextruded material. *J Polym Environ* 11:169–179
38. Da Silva KIM, Fernandes JA, Kohlrausch EC, Dupont J, Santos MJL, Gil MP (2014) Structural stability of photodegradable poly(L-lactic acid)/PE/TiO<sub>2</sub> nanocomposites through TiO<sub>2</sub> nanospheres and TiO<sub>2</sub> nanotubes incorporation. *Polym Bull* 71:1205–1217. doi:[10.1007/s00289-014-1119-0](https://doi.org/10.1007/s00289-014-1119-0)
39. Meng B, Tao J, Deng J, Wu Z, Yang M (2011) Toughening of polylactide with higher loading of nano-titania particles coated by poly( $\epsilon$ -caprolactone). *Mater Lett* 65:729–732. doi:[10.1016/j.matlet.2010.11.029](https://doi.org/10.1016/j.matlet.2010.11.029)
40. Buzarovska A (2013) PLA nanocomposites with functionalized TiO<sub>2</sub> nanoparticles. *Polym Plast Technol Eng* 52:280–286. doi:[10.1080/03602559.2012.751411](https://doi.org/10.1080/03602559.2012.751411)
41. Chen C, Lv G, Pan C, Song M, Wu C, Guo D, Wang X, Chen B, Gu Z (2007) Poly(lactic acid) (PLA) based nanocomposites—a novel way of drug-releasing. *Biomed Mater* 2:L1–L4
42. Luo YB, Wang XL, Xu DY, Wang YZ (2009) Preparation and properties of nanocomposites based on poly(lactic acid) and functionalized TiO<sub>2</sub>. *Acta Mater* 57:3182–3191. doi:[10.1016/j.actamat.2009.03.022](https://doi.org/10.1016/j.actamat.2009.03.022)
43. Li Y, Chen C, Li J, Sun XS (2011) Synthesis and characterization of bionanocomposites of poly(lactic acid) and TiO<sub>2</sub> nanowires by in situ polymerization. *Polymer* 52:2367–2375. doi:[10.1016/j.polymer.2011.03.050](https://doi.org/10.1016/j.polymer.2011.03.050)
44. Evora VMF, Shukla A (2003) Fabrication, characterization, and dynamic behavior of polyester/TiO<sub>2</sub> nanocomposites. *Mater Sci Eng* 361:358–366. doi:[10.1016/S0921-5093\(03\)00536-7](https://doi.org/10.1016/S0921-5093(03)00536-7)
45. Cho J, Denes FS, Timmons RB (2006) Plasma processing approach to molecular surface tailoring of nanoparticles: improved photocatalytic activity of TiO<sub>2</sub>. *Chem Mater* 18:2989–2996. doi:[10.1021/cm060212g](https://doi.org/10.1021/cm060212g)
46. Degreee P, Dubois P, Jérôme R (1997) Bulk polymerization of lactides initiated by aluminum isopropoxide. I. Mechanism and kinetics. *Macromol Symp* 123:67–84. doi:[10.1002/masy.19971230108](https://doi.org/10.1002/masy.19971230108)
47. Lee SJ, Han SW, Kim K (2002) Perfluorocarbon-stabilized silver nanoparticles manufactured from layered silver carboxylates. *Chem Commun* 5:442–443. doi:[10.1039/B111607J](https://doi.org/10.1039/B111607J)

48. O'Donnell A, Yach K, Reven L (2008) Particle–particle interactions and chain dynamics of fluorocarbon and hydrocarbon Functionalized ZrO<sub>2</sub> nanoparticles. *Langmuir* 24:2465–2471. doi:[10.1021/la702503m](https://doi.org/10.1021/la702503m)
49. Bezrodna T, Puchkovska G, Shimanovska V, Chashecnikova I, Khalyavka T, Baran J (2003) Pyridine–TiO<sub>2</sub> surface interaction as a probe for surface active centers analysis. *Appl Surf Sci* 214:222–231. doi:[10.1016/S0169-4332\(03\)00346-5](https://doi.org/10.1016/S0169-4332(03)00346-5)
50. Pluta M, Galeski A, Alexandre M, Paul MA, Dubois P (2002) Poly(lactide)/montmorillonite nanocomposites and microcomposites prepared by melt blending: structure and some physical properties. *J Appl Polym Sci* 86:1497–1506. doi:[10.1002/app.11309](https://doi.org/10.1002/app.11309)
51. Ray SS, Yamada K, Okamoto M, Ueda K (2003) New poly(lactide)-layered silicate nanocomposites. 2. Concurrent improvements of material properties, biodegradability and melt rheology. *Polymer* 44:857–866. doi:[10.1016/S0032-3861\(02\)00818-2](https://doi.org/10.1016/S0032-3861(02)00818-2)
52. Ray SS, Yamada K, Okamoto M, Ueda K (2002) New poly(lactide)/layered silicate nanocomposite: nanoscale control over multiple properties. *Macromol Rapid Commun* 23:943–947. doi:[10.1002/1521-3927\(200211\)23:16<943:AID-MARC943>3.0.CO;2-F](https://doi.org/10.1002/1521-3927(200211)23:16<943:AID-MARC943>3.0.CO;2-F)
53. Xiaoyan P, Yi C, Xueming M, Lihui ZJ (2004) Phase transformation of nanocrystalline anatase powders induced by mechanical activation. *J Am Ceram Soc* 87:1164–1166. doi:[10.1111/j.1551-2916.2004.01164.x](https://doi.org/10.1111/j.1551-2916.2004.01164.x)
54. Yan SF, Yin JB, Yang Y, Dai ZZ, Ma J, Chen XS (2007) Surface-grafted silica linked with l-lactic acid oligomer: a novel nanofiller to improve the performance of biodegradable poly(l-lactide). *Polymer* 48:1688–1694. doi:[10.1016/j.polymer.2007.01.037](https://doi.org/10.1016/j.polymer.2007.01.037)
55. Ogata N, Jimenez G, Kawai H, Ogihara TJ (1997) Structure and thermal/mechanical properties of poly(l-lactide)–clay blend. *Polym Sci Part B Polym Phys* 35:389–396. doi:[10.1002/\(SICI\)1099-0488\(19970130\)35:2<389:AID-POLB14>3.0.CO;2-E](https://doi.org/10.1002/(SICI)1099-0488(19970130)35:2<389:AID-POLB14>3.0.CO;2-E)
56. Di Lorenzo ML, Cocca M, Malinconico M (2011) Crystal polymorphism of poly(l-lactic acid) and its influence on thermal properties. *Termochim Acta* 522:110–117. doi:[10.1016/j.tca.2010.12.027](https://doi.org/10.1016/j.tca.2010.12.027)
57. Tsai CC, Wu RJ, Cheng XY, Li SC, Siao YY, Kong DC, Jang GW (2010) Crystallinity and dimensional stability of biaxial oriented poly(lactic acid) films. *Polym Degrad Stab* 95:1292–1298. doi:[10.1016/j.polymdegradstab.2010.02.032](https://doi.org/10.1016/j.polymdegradstab.2010.02.032)
58. Najafi N, Heuzey MC, Carreau PJ, Wood-Adams PM (2012) Control of thermal degradation of poly(lactide) (PLA)–clay nanocomposites using chain extenders. *Polym Degrad Stab* 97:554–565. doi:[10.1016/j.polymdegradstab.2012.01.016](https://doi.org/10.1016/j.polymdegradstab.2012.01.016)
59. Han L, Han C, Cao W, Wang X, Bian J, Dong L (2012) Preparation and characterization of biodegradable poly(3-hydroxybutyrate-co-4-hydroxybutyrate)/silica nanocomposites. *Polym Eng Sci* 52:250–258. doi:[10.1002/pen.22076](https://doi.org/10.1002/pen.22076)
60. Kusmono, Mohd Ishak ZA, Chow WS, Takeichi T, Rochmadi (2010) Effect of clay modification on the morphological, mechanical, and thermal properties of polyamide 6/polypropylene/montmorillonite nanocomposites. *Polym Comp* 31:1156–1167. doi:[10.1002/pc.20902](https://doi.org/10.1002/pc.20902)
61. Díez-Pascual AM, Díez-Vicente AL (2014) Poly(3-hydroxybutyrate)/ZnO bionanocomposites with improved mechanical, barrier and antibacterial properties. *Int J Mol Sci* 15:10950–10973. doi:[10.3390/ijms150610950](https://doi.org/10.3390/ijms150610950)
62. Paula MP, Alexandra M, Degée P, Henricc C, Rulmont A, Dubois P (2003) New nanocomposite materials based on plasticized poly(l-lactide) and organo-modified montmorillonites: thermal and morphological study. *Polymer* 44:443–450. doi:[10.1016/S0032-3861\(02\)00778-4](https://doi.org/10.1016/S0032-3861(02)00778-4)
63. Chang JH, An YU, Sur GSJ (2003) Poly(lactic acid) nanocomposites with various organoclays. I. Thermomechanical properties, morphology and gas permeability. *Polym Sci Part B Polym Phys* 41:94–103. doi:[10.1002/polb.10349](https://doi.org/10.1002/polb.10349)
64. Bocchini S, Fukushima K, Di Blasio A, Fina A, Frache A, Geobaldo F (2010) Poly(lactic acid) and poly(lactic acid)-based nanocomposite photooxidation. *Biomacromolecules* 11:2919–2926. doi:[10.1021/bm1006773](https://doi.org/10.1021/bm1006773)